

See discussions, stats, and author profiles for this publication at: <https://www.researchgate.net/publication/375695028>

GFANC-Kalman: Generative Fixed-Filter Active Noise Control with CNN-Kalman Filtering

Article in *Signal Processing Letters, IEEE* · November 2023

DOI: 10.1109/LSP.2023.3334695

CITATIONS

5

READS

393

5 authors, including:



Zhengding Luo

Nanyang Technological University

35 PUBLICATIONS 213 CITATIONS

SEE PROFILE



Dongyuan Shi

Nanyang Technological University

123 PUBLICATIONS 1,482 CITATIONS

SEE PROFILE



Xiaoyi Shen

Nanyang Technological University

42 PUBLICATIONS 459 CITATIONS

SEE PROFILE








Junwei Ji

Nanyang Technological University

18 PUBLICATIONS 71 CITATIONS

SEE PROFILE

GFANC-Kalman: Generative Fixed-Filter Active Noise Control With CNN-Kalman Filtering

Zhengding Luo , *Graduate Student Member, IEEE*, Dongyuan Shi , *Senior Member, IEEE*,
Xiaoyi Shen , *Member, IEEE*, Junwei Ji , *Graduate Student Member, IEEE*,
and Woon-Seng Gan , *Senior Member, IEEE*

Abstract—Selective Fixed-filter Active Noise Control (SFANC) is limited by its selection of a single candidate from pre-trained control filters. In contrast, Generative Fixed-filter Active Noise Control (GFANC) addresses this limitation by employing an adaptive combination of sub control filters to generate more suitable control filters for different primary noises. However, GFANC solely relies on the information from the current noise frame to generate its control filter, resulting in potential inaccuracies when dealing with dynamic noises. Therefore, we propose a GFANC-Kalman approach that integrates an efficient one-dimensional convolutional neural network (1D CNN) with a Kalman filter to further improve the performance of GFANC. Specifically, the weight vector used to combine sub control filters is predicted by the 1D CNN for each noise frame, and then processed by the Kalman filter with minimal complexity. By considering the correlation between adjacent noise frames, the Kalman filter can enhance the accuracy and robustness of weight vector prediction. Hence, GFANC-Kalman is more able to adapt to changes in noise distribution, particularly for dynamic noises. Numerical simulations validate the efficacy of the proposed GFANC-Kalman approach in dealing with real-world dynamic noises.

Index Terms—CNN-Kalman filtering, dynamic noise cancellation, fixed-filter active noise control, generative ANC.

I. INTRODUCTION

THE rapid increase of industrial equipment utilized for ventilation, air circulation, power transformation, and pressurization etc., has resulted in the emergence of acoustic noise problems [1], [2], [3]. Conventional passive sound absorbers, such as fiberglass or foam panels, are ineffective and impractical for attenuating low-frequency noises [4], [5], [6]. A more effective approach can be provided by active noise control (ANC), which produces an anti-noise with equal magnitude and opposite phase to suppress the unwanted noise [7], [8], [9], [10], [11]. Due to its compact size and proven ability to attenuate low-frequency noises, ANC has found extensive applications in various commercial products including windows, headphones, headrests, and vehicles [12], [13], [14].

Manuscript received 3 July 2023; accepted 13 November 2023. Date of publication 20 November 2023; date of current version 17 January 2024. The associate editor coordinating the review of this manuscript and approving it for publication was Dr. Yu Tsao. (Corresponding author: Dongyuan Shi.)

The authors are with the School of Electrical and Electronic Engineering, Nanyang Technological University, Singapore 639 798 (e-mail: luoz0021@e.ntu.edu.sg; dongyuan.shi@ntu.edu.sg; xiaoyi003@e.ntu.edu.sg; junwei002@e.ntu.edu.sg; ewsgan@ntu.edu.sg).

The paper code is available at <https://github.com/Luo-Zhengding/GFANC-Kalman>.

Digital Object Identifier 10.1109/LSP.2023.3334695

In traditional ANC systems, the filtered reference least mean square (FxLMS) algorithm and its derivatives have gained popularity, which can compensate for secondary path delays and achieve high computational efficiency [15], [16], [17]. However, adaptive algorithms are less efficient at coping with rapidly varying or dynamic disturbances because of their slow convergence and weak tracking abilities [18], [19], [20]. Many ANC products have opted for fixed-filter ANC algorithms to improve response time and robustness. Nevertheless, fixed control filters may result in a potential decline when controlling other types of noises because they are only appropriate for specific noise types [21], [22], [23].

Convolutional neural networks (CNNs) and other deep learning techniques have emerged as effective approaches for enhancing fixed-filter ANC methods [24], [25], [26], [27]. A deep learning-based SFANC technique that employs CNNs to choose appropriate pre-trained control filters for primary noises was proposed by Shi et al. [28]. Its parameters can be learned automatically from noise datasets without further manual intervention. Nevertheless, the limited quantity of pre-trained control filters in SFANC may lead to unsatisfactory performance in attenuating some noises, particularly those that differ much from the filter-training noises. In a prior study, a generative fixed-filter ANC (GFANC) technique was introduced [29] to address the limitation of SFANC by the generation of suitable control filters for different noises.

The GFANC approach [29] can generate various control filters by adaptively combining sub control filters that are decomposed from a pre-trained broadband control filter. However, GFANC estimates the weight vector used to combine sub control filters solely using information from the current noise frame. This approach may result in erroneous weight vector estimations, especially for rapidly varying or dynamic noises, which would degrade the noise reduction performance. To alleviate this issue, an alternative method that incorporates temporal dependencies and adapts to changes in noise distribution is required.

Therefore, this paper proposes a GFANC-Kalman method, which leverages CNN's strong feature extraction capabilities and the robust estimation abilities of Kalman filtering [30], [31]. The GFANC-Kalman algorithm estimates the weight vector used for combining sub control filters by integrating a lightweight one-dimensional CNN (1D CNN) and a Kalman filter. Utilizing the Kalman filter, the GFANC-Kalman takes advantage of the temporal correlation between successive noise frames, resulting in a more precise weight vector estimation. Moreover, the Kalman filter has a low computational complexity, which enhances the applicability of this technique. Experimental results on real-world dynamic noises suggest that GFANC-Kalman can

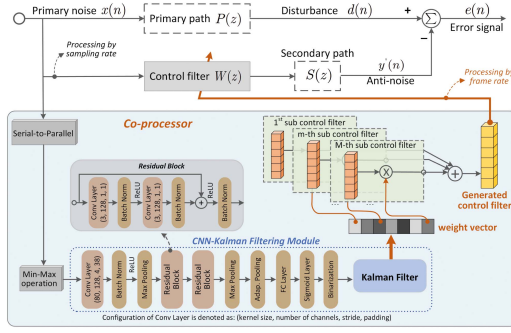


Fig. 1. Proposed GFANC-Kalman approach mainly consists of two modules: The generation of control filters in the co-processor and noise cancellation in the real-time controller. The temporal correlation between adjacent noise frames is considered in the CNN-Kalman filtering module.

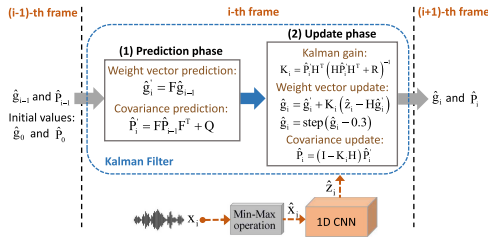


Fig. 2. Block diagram of the CNN-Kalman filtering module, where the weight vector \hat{g}_i of i -th frame noise is predicted based on the information from the current frame and the previous frame. Noticeably, the Kalman filter exhibits linear computations within this module.

achieve better noise reduction levels and robustness compared to GFANC [29] and SFANC [28].

II. THE GFANC-KALMAN APPROACH

The block diagram of the proposed GFANC-Kalman approach is illustrated in Fig. 1. Given each frame of noise, the co-processor generates a corresponding control filter using the inner product of a weight vector and sub control filters. As Fig. 2 shows, the weight vector is estimated by the integrated CNN-Kalman filtering module. Notably, the generation of control filters is executed on a co-processor (like a laptop) at the frame rate, while real-time noise control is performed at the sampling rate. The efficient coordination between the co-processor and real-time controller enables delayless processing, making GFANC-Kalman a promising solution for practical ANC applications.

A. Sub Control Filters

Before using the GFANC-Kalman approach, we need to obtain the sub control filters for generating new control filters. To achieve this, we employed a practical filter decomposition method based on filter perfect-reconstruction theory [32]. Initially, we utilized the target ANC system to cancel a broadband primary noise, whose frequency band contained the frequency components of interest.

The optimal control filter derived by the FxLMS algorithm [33] serves as the pre-trained broadband control filter, which is the sole required prior data. We assume that the pre-trained control filter has N taps and is represented by the

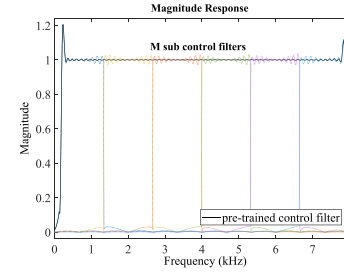


Fig. 3. Frequency spectrum of the pre-trained broadband control filter (black line) and its sub control filters (colored lines) in GFANC-Kalman.

vector \mathbf{c} . By applying Discrete Fourier Transform (DFT), its frequency spectrum is computed as

$$\mathbf{C} = \mathbf{F}_N \mathbf{c}, \quad (1)$$

where \mathbf{F}_N represents the DFT matrix. In frequency domain, the control filter \mathbf{C} can be divided into M sub control filters, which is expressed as

$$\mathbf{C} = \sum_{m=1}^M \mathbf{C}_m, \quad (2)$$

where \mathbf{C}_m denotes the frequency spectrum of the m -th sub control filter. The bandwidth of each sub control filter is $I = \lfloor \frac{N}{2M} \rfloor$. The time-domain representation of the m -th sub control filter is obtained from

$$\mathbf{c}_m = \mathbf{F}_N^{-1} \mathbf{C}_m, \quad (3)$$

where \mathbf{F}_N^{-1} denotes the inverse DFT matrix.

As demonstrated in [29], the control filter \mathbf{c} can be perfectly reconstructed in the time domain by all of its sub control filters:

$$\mathbf{c} = \sum_{m=1}^M \mathbf{c}_m. \quad (4)$$

Consequently, M sub control filters shown in Fig. 3 serve as the orthogonal base for generating new control filters in the GFANC-Kalman method.

B. CNN-Kalman Filtering Module

When generating the weight vector used for combining sub control filters, the 1D CNN and Kalman filter are integrated as a CNN-Kalman filtering module. Incorporating the recursive nature of the Kalman model [34] and the highly nonlinear transformation capability of CNN benefits from both model-based and learning-based methods.

1) *1D CNN*: Recent studies have demonstrated that CNNs using time-domain waveforms can perform comparably to those employing frequency spectrograms in audio applications [35]. Given the practicality and convenience of using time-domain data, a lightweight 1D CNN is implemented in the co-processor. Each one-second noise waveform is normalized and used as the input of the 1D CNN [36].

The proposed 1D CNN, as depicted in Fig. 1, uses convolutional kernels of varying sizes to simulate a variety of bandpass filters for extracting features from the noise signal effectively [37]. Sub control filters are combined using binary weights, where each weight is either 0 or 1, to reduce memory and computation resources. The task of obtaining binary weights can be treated as a multi-label classification problem [38]. To

train the 1D CNN for this task, the Sigmoid function and Binary Cross Entropy (BCE) loss are employed.

2) *Kalman Filter*: Assuming linear system and Gaussian errors, Kalman filters can optimally estimate the system state [39], [40]. Kalman filters are light on memory and very fast, making them well-suited for real-time embedded systems [41], [42]. In this case, the system state refers to the weight vector. In the GFANC-Kalman method, the weight vector for each noise frame can be modelled as a first-order Markov chain [43], which means that the weight vector for the next frame only depends on the current weight vector.

To use the Kalman filtering module to estimate the weight vector based on the previous state and the current measurement, it is assumed that the noise in the system is Gaussian and has a certain statistical distribution. More precisely, the state \mathbf{g}_i and measurement \mathbf{z}_i can be represented as

$$\begin{aligned}\mathbf{g}_i &= \mathbf{F}\mathbf{g}_{i-1} + \mathbf{h}, \quad \mathbf{h} \sim N(\mathbf{0}, \mathbf{Q}), \\ \mathbf{z}_i &= \mathbf{H}\mathbf{g}_i + \mathbf{v}, \quad \mathbf{v} \sim N(\mathbf{0}, \mathbf{R}),\end{aligned}\quad (5)$$

where \mathbf{g}_i and \mathbf{g}_{i-1} are the state of the current frame i and the previous frame $i - 1$. \mathbf{F} and \mathbf{H} denote the state transition matrix and measurement matrix, respectively. The process noise \mathbf{h} has a normal distribution with covariance \mathbf{Q} , and the measurement noise \mathbf{v} has a normal distribution with covariance \mathbf{R} .

The Kalman filtering module can yield the best estimate $\hat{\mathbf{g}}_i$ to minimize the mean of the squared error through two iterative steps: prediction and update, as illustrated in Fig. 2. The initial state $\hat{\mathbf{g}}_0$ and its error covariance matrix $\hat{\mathbf{P}}_0$ are set to a zero vector and an identity matrix, respectively.

For the prediction phase, the current state and its error covariance matrix are estimated given the previous state:

$$\begin{aligned}\hat{\mathbf{g}}'_i &= \mathbf{F}\hat{\mathbf{g}}_{i-1}, \\ \hat{\mathbf{P}}'_i &= \mathbf{F}\hat{\mathbf{P}}_{i-1}\mathbf{F}^T + \mathbf{Q}.\end{aligned}\quad (6)$$

During the update step, the optimal Kalman gain \mathbf{K}_i is calculated. This gain is utilized with the current measurement $\hat{\mathbf{z}}'_i$ to update the predicted state and its error covariance matrix.

$$\begin{aligned}\mathbf{K}_i &= \hat{\mathbf{P}}'_i \mathbf{H}^T (\mathbf{H} \hat{\mathbf{P}}'_i \mathbf{H}^T + \mathbf{R})^{-1}, \\ \hat{\mathbf{g}}_i &= \hat{\mathbf{g}}'_i + \mathbf{K}_i (\hat{\mathbf{z}}'_i - \mathbf{H} \hat{\mathbf{g}}'_i), \\ \hat{\mathbf{P}}_i &= (\mathbf{I} - \mathbf{K}_i \mathbf{H}) \hat{\mathbf{P}}'_i.\end{aligned}\quad (7)$$

In the equation, \mathbf{I} denotes the identity matrix, and the observed measurement $\hat{\mathbf{z}}'_i$ means the binarized output of the 1D CNN given the i -th frame noise \mathbf{x}_i :

$$\begin{aligned}\hat{\mathbf{z}}_i &= \text{CNN}(\mathbf{x}_i), \\ \hat{\mathbf{z}}'_i &= \text{step}(\hat{\mathbf{z}}_i - 0.3),\end{aligned}\quad (8)$$

where $\text{CNN}(\cdot)$ denotes the operation of the pre-trained 1D CNN model. $\text{step}(\cdot)$ represents a step function that binarizes the value by comparing it with a threshold value of 0.3. Finally, the $\hat{\mathbf{g}}_i$ estimated by the Kalman filter is also binarized using the same step function.

The computational complexity of the Kalman filter is presented in Table I in terms of multipliers and additions. For each noise frame, the state vector and measurement vector are one-dimensional weight vectors with M values. \mathbf{R} , \mathbf{F} , and \mathbf{H} are all identity matrices, and \mathbf{Q} is a 0.5-filled diagonal matrix. Therefore, this Kalman filter exhibits linear complexity, significantly reducing the computational burden.

TABLE I
COMPUTATION COMPLEXITY OF KALMAN FILTERING MODULE

| Algorithm | #Multiplier | #Addition |
|-------------------------------|-------------|-----------|
| Kalman filter in GFANC-Kalman | $3M$ | $5M$ |

M denotes the number of sub control filters.

TABLE II
PERFORMANCE COMPARISON OF DIFFERENT 1D NETWORKS

| Network | Test Accuracy | #Parameters |
|----------------------|---------------|-------------|
| Proposed 1D CNN | 96.50% | 0.21M |
| DenseNet [44] | 95.95% | 0.48M |
| M3 Network [45] | 93.55% | 0.22M |
| M5 Network [45] | 96.15% | 0.56M |
| M11 Network [45] | 95.05% | 1.79M |
| M18 Network [45] | 95.09% | 3.69M |
| M34-res Network [45] | 96.29% | 3.99M |

C. Real-Time Noise Cancellation

Given i -th frame noise, the corresponding weight vector $\hat{\mathbf{g}}_i$ is estimated by the CNN-Kalman filtering module. Based on the weight vector, M sub control filters are summed together to generate a control filter $\mathbf{w}(n)$ in the co-processor:

$$\begin{aligned}\mathbf{w}(n) &= \sum_{m=1}^M \hat{g}_i^m \mathbf{c}_m(n), \\ \hat{\mathbf{g}}_i &= [\hat{g}_i^1, \dots, \hat{g}_i^m, \dots, \hat{g}_i^M],\end{aligned}\quad (9)$$

where n denotes the time index. The combination weight of the m -th sub control filter $\mathbf{c}_m(n)$ is represented by \hat{g}_i^m .

Subsequently, the generated control filter is provided to the real-time controller for noise cancellation at the sampling rate. The error signal is computed as

$$e(n) = d(n) - \mathbf{x}^T(n) \mathbf{w}(n) * s(n), \quad (10)$$

where $\mathbf{x}(n)$ and $d(n)$ denote the reference signal and the disturbance, respectively. The secondary path's impulse response is denoted by $s(n)$. $*$ represents linear convolution operation. The error signal is only measured to assess the noise reduction performance of GFANC-Kalman, rather than being utilized for updating the control filter as done in adaptive algorithms.

III. NUMERICAL SIMULATIONS

The GFANC-Kalman approach's effectiveness is evaluated through some numerical simulations. In terms of experimental setup, the number of sub control filters M is set to 15. The sampling rate and control filter's length are set to 16 kHz and 1,024 taps, respectively. In the simulations, synthetic bandpass filters with a frequency range of 20–7,980 Hz are used as the primary path and secondary path.

A. Effectiveness of the Proposed 1D CNN

A synthetic noise dataset is split into three subsets for training the network: 80,000 noise instances for training, 2,000 instances for validation, and the remaining 2,000 instances for testing. White noise is filtered through several bandpass filters with arbitrary center frequencies and bandwidths to create the noise instances. The duration of each noise instance is 1 s. Instead of manual labelling, the adaptive labelling mechanism [29] is employed to assign optimal weight vectors to the noise instances.

The proposed 1D CNN is compared against some other benchmark networks. Table II provides a summary of the comparison results, where test accuracy is defined as the accuracy of weight

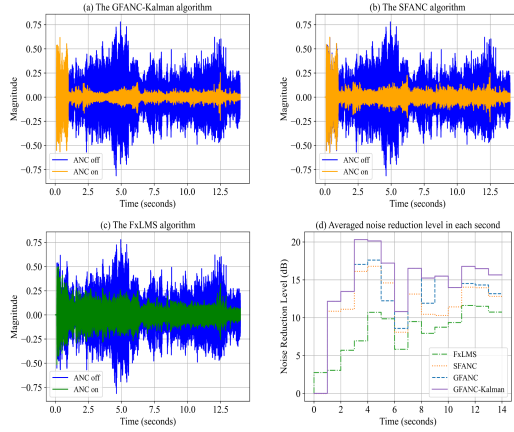


Fig. 4. (a)–(c): Noise reduction results of different ANC algorithms, (d): Averaged noise reduction level in each second, on the street noise.

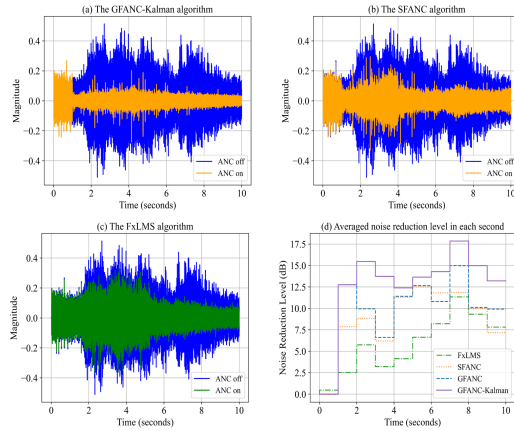


Fig. 5. (a)–(c): Noise reduction results of different ANC algorithms, (d): Averaged noise reduction level in each second, on the trolley noise.

vector predictions in the testing dataset. It is observed that the highest prediction accuracy of 96.50% is achieved by the proposed 1D CNN, demonstrating its ability to efficiently extract noise features and estimate appropriate weight vectors. Additionally, the proposed 1D CNN is a lightweight network with only 0.21 M parameters, which is easy to deploy for practical ANC applications.

B. Noise Cancellation on Real Noises

The GFANC-Kalman method is compared to GFANC [29], SFANC [46], and FxLMS for reducing real dynamic noises that are not included in the training dataset. The step size of the FxLMS algorithm is 0.0001 to avoid divergence. Figs. 4 and 5 depict the noise reduction results for the street and trolley noises using different ANC techniques.

According to Figs. 4 and 5, GFANC-Kalman consistently outperforms GFANC on the two noises. For the street noise and trolley noise, the averaged noise reduction levels achieved by GFANC-Kalman are up to 5 dB and 7 dB higher than those achieved by GFANC, respectively. This indicates that the Kalman filter contributes to better noise reduction performance with the temporal correlation between adjacent frames. Additionally, GFANC-Kalman is superior to SFANC in terms of noise reduction level due to its ability to generate more appropriate

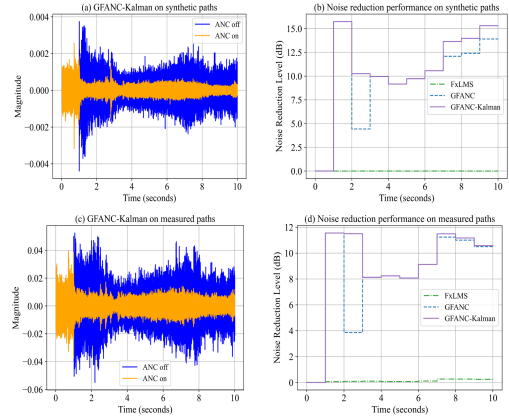


Fig. 6. (a) and (b): Noise reduction performance on synthetic paths, (c) and (d): Noise reduction performance on measured paths, when dealing with the drill noise.

control filters. Also, GFANC-Kalman can respond to the noises much faster than FxLMS. However, GFANC-Kalman, GFANC, and SFANC are incapable of handling noises during the initial 1 s.

C. Noise Cancellation on Measured Acoustic Paths

In the preceding simulations, synthetic filters were used as primary and secondary paths to make the adjustment process more accessible. During evaluation, the acoustic paths were assumed to be the same as those used during training. In this section, however, real acoustic paths measured from a noise chamber's vent are utilized to evaluate the transferability of the GFANC-Kalman method. On the measured acoustic paths, corresponding sub control filters are obtained by the decomposition of a new pre-trained broadband control filter, while keeping the CNN-Kalman filtering module unchanged.

The noise reduction results on the synthetic and measured acoustic paths are shown in Fig. 6, with the primary noise being a drill noise. Fig. 6 suggests that GFANC-Kalman attenuates the drill noise more effectively than GFANC on the measured acoustic paths, proving its superiority over GFANC. GFANC-Kalman and GFANC used on the measured acoustic paths exhibit a slight degradation in noise reduction levels compared to those used on synthetic acoustic paths. In contrast, the FxLMS algorithm performs poorly when dealing with the noise's rapid variation. Therefore, the GFANC-Kalman method exhibits good robustness and transferability on the real acoustic paths.

IV. CONCLUSION

This letter proposes a GFANC-Kalman method for enhancing GFANC with minimal computational overhead introduced by the Kalman filter. The proposed method incorporates a CNN-Kalman filtering module that automatically estimates the weight vector for combining sub control filters. With the recursive nature of Kalman filtering and the representation learning capability of CNN, this method achieves better weight vector estimation by considering the correlation between adjacent noise frames. Experiments on real dynamic noises indicate that GFANC-Kalman achieves a higher level of noise cancellation than GFANC, SFANC, and FxLMS. Moreover, GFANC-Kalman exhibits good robustness and transferability when evaluated on real acoustic paths.

REFERENCES

- [1] S. M. Kuo and D. R. Morgan, "Active noise control: A tutorial review," *Proc. IEEE*, vol. 87, no. 6, pp. 943–973, Jun. 1999.
- [2] S. J. Elliott and P. A. Nelson, "Active noise control," *IEEE Signal Process. Mag.*, vol. 10, no. 4, pp. 12–35, Oct. 1993.
- [3] C. N. Hansen, *Understanding Active Noise Cancellation*. Boca Raton, FL, USA: CRC Press, 2002.
- [4] T. Schumacher, H. Krüger, M. Jeub, P. Vary, and C. Beaugeant, "Active noise control in headsets: A new approach for broadband feedback ANC," in *Proc. IEEE Int. Conf. Acoust., Speech Signal Process.*, 2011, pp. 417–420.
- [5] Y. Kajikawa, W.-S. Gan, and S. M. Kuo, "Recent advances on active noise control: Open issues and innovative applications," *APSIPA Trans. Signal Inf. Process.*, vol. 1, 2012, Art. no. e3.
- [6] M. Pawelczyk, "Analogue active noise control," *Appl. Acoust.*, vol. 63, no. 11, pp. 1193–1213, 2002.
- [7] H. Zhang, A. Pandey, and D. L. Wang, "Low-latency active noise control using attentive recurrent network," *IEEE/ACM Trans. Audio, Speech, Lang. Process.*, vol. 31, pp. 1114–1123, 2023.
- [8] Y. Wang, Z. Lan, X. Wu, and T. Qu, "TT-Net: Dual-path transformer based sound field translation in the spherical harmonic domain," in *Proc. IEEE Int. Conf. Acoust., Speech Signal Process.*, 2023, pp. 1–5.
- [9] J. A. Zhang, N. Murata, Y. Maeno, P. N. Samarasinghe, T. D. Abhayapala, and Y. Mitsufuji, "Coherence-based performance analysis on noise reduction in multichannel active noise control systems," *J. Acoustical Soc. Amer.*, vol. 148, no. 3, pp. 1519–1528, 2020.
- [10] N. Han and X. Qiu, "A study of sound intensity control for active noise barriers," *Appl. Acoust.*, vol. 68, no. 10, pp. 1297–1306, 2007.
- [11] C.-Y. Chang, C.-T. Chuang, S. M. Kuo, and C.-H. Lin, "Multi-functional active noise control system on headrest of airplane seat," *Mech. Syst. Signal Process.*, vol. 167, 2022, Art. no. 108552.
- [12] H. Sun, J. Zhang, T. Abhayapala, and P. Samarasinghe, "Spatial active noise control with the remote microphone technique: An approach with a moving higher order microphone," in *Proc. IEEE Int. Conf. Acoust., Speech Signal Process.*, 2022, pp. 8707–8711.
- [13] Y. Xiao and J. Wang, "A new feedforward hybrid active noise control system," *IEEE Signal Process. Lett.*, vol. 18, no. 10, pp. 591–594, Oct. 2011.
- [14] D. Chen, L. Cheng, D. Yao, J. Li, and Y. Yan, "A secondary path-decoupled active noise control algorithm based on deep learning," *IEEE Signal Process. Lett.*, vol. 29, pp. 234–238, 2022.
- [15] R. Gupta et al., "Augmented/mixed reality audio for hearables: Sensing, control, and rendering," *IEEE Signal Process. Mag.*, vol. 39, no. 3, pp. 63–89, May 2022.
- [16] F. Yang, J. Guo, and J. Yang, "Stochastic analysis of the filtered-x LMS algorithm for active noise control," *IEEE/ACM Trans. Audio, Speech, Lang. Process.*, vol. 28, pp. 2252–2266, 2020.
- [17] X. Shen, D. Shi, Z. Luo, J. Ji, and W.-S. Gan, "A momentum two-gradient direction algorithm with variable step size applied to solve practical output constraint issue for active noise control," in *Proc. IEEE Int. Conf. Acoust., Speech Signal Process.*, 2023, pp. 1–5.
- [18] S. Liebich, P. Jax, and P. Vary, "Active cancellation of the occlusion effect in hearing aids by time invariant robust feedback," in *Proc. Speech Commun.; 12. ITG Symp.*, 2016, pp. 1–5.
- [19] J. Cheer and S. J. Elliott, "Multichannel control systems for the attenuation of interior road noise in vehicles," *Mech. Syst. Signal Process.*, vol. 60/61, pp. 753–769, 2015.
- [20] C. Shi, F. Du, and Q. Wu, "A digital twin architecture for wireless networked adaptive active noise control," *IEEE/ACM Trans. Audio, Speech, Lang. Process.*, vol. 30, pp. 2768–2777, 2022.
- [21] D. Shi, W.-S. Gan, B. Lam, and K. Ooi, "Fast adaptive active noise control based on modified model-agnostic meta-learning algorithm," *IEEE Signal Process. Lett.*, vol. 28, pp. 593–597, 2021.
- [22] P. R. Benois, R. Roden, M. Blau, and S. Doclo, "Optimization of a fixed virtual sensing feedback ANC controller for in-ear headphones with multiple loudspeakers," in *Proc. IEEE Int. Conf. Acoust., Speech Signal Process.*, 2022, pp. 8717–8721.
- [23] C. Shi, R. Xie, N. Jiang, H. Li, and Y. Kajikawa, "Selective virtual sensing technique for multi-channel feedforward active noise control systems," in *Proc. IEEE Int. Conf. Acoust., Speech Signal Process.*, 2019, pp. 8489–8493.
- [24] D. Shi, W.-S. Gan, B. Lam, and S. Wen, "Feedforward selective fixed-filter active noise control: Algorithm and implementation," *IEEE/ACM Trans. Audio, Speech, Lang. Process.*, vol. 28, pp. 1479–1492, 2020.
- [25] Z. Luo, D. Shi, J. Ji, and W.-s. Gan, "Implementation of multi-channel active noise control based on back-propagation mechanism," 2022, *arXiv:2208.08086*.
- [26] S.-W. Fu, C.-F. Liao, and Y. Tsao, "Learning with learned loss function: Speech enhancement with quality-net to improve perceptual evaluation of speech quality," *IEEE Signal Process. Lett.*, vol. 27, pp. 26–30, 2020.
- [27] H. Zhang and D. Wang, "Deep ANC: A deep learning approach to active noise control," *Neural Netw.*, vol. 141, pp. 1–10, 2021.
- [28] D. Shi, B. Lam, K. Ooi, X. Shen, and W.-S. Gan, "Selective fixed-filter active noise control based on convolutional neural network," *Signal Process.*, vol. 190, 2022, Art. no. 108317.
- [29] Z. Luo, D. Shi, X. Shen, J. Ji, and W.-S. Gan, "Deep generative fixed-filter active noise control," in *Proc. IEEE Int. Conf. Acoust., Speech Signal Process.*, 2023, pp. 1–5.
- [30] C. K. Chui and G. Chen, *Kalman Filtering*. Berlin, Germany: Springer, 2017.
- [31] Y. Chen, D. Zhao, and H. Li, "Deep Kalman filter with optical flow for multiple object tracking," in *Proc. IEEE Int. Conf. Syst., Man Cybern.*, 2019, pp. 3036–3041.
- [32] H. H. Dam, S. Nordholm, A. Cantoni, and J. M. d. Haan, "Iterative method for the design of DFT filter bank," *IEEE Trans. Circuits Syst. II: Exp. Briefs*, vol. 51, no. 11, pp. 581–586, Nov. 2004.
- [33] S. M. Kuo and D. R. Morgan, *Active Noise Control Systems*, vol. 4. Wiley, New York, NY, USA, 1996.
- [34] R. E. Kalman, "A new approach to linear filtering and prediction problems," *J. Basic Eng.*, vol. 82, no. 1, pp. 35–45, 1960.
- [35] Y. Hoshen, R. J. Weiss, and K. W. Wilson, "Speech acoustic modeling from raw multichannel waveforms," in *Proc. IEEE Int. Conf. Acoust., Speech Signal Process.*, 2015, pp. 4624–4628.
- [36] D. Shi, W.-S. Gan, B. Lam, Z. Luo, and X. Shen, "Transferable latent of CNN-based selective fixed-filter active noise control," *IEEE/ACM Trans. Audio, Speech, Lang. Process.*, vol. 31, pp. 2910–2921, 2023.
- [37] K. He, X. Zhang, S. Ren, and J. Sun, "Deep residual learning for image recognition," in *Proc. IEEE Conf. Comput. Vis. Pattern Recognit.*, 2016, pp. 770–778.
- [38] C.-K. Yeh, W.-C. Wu, W.-J. Ko, and Y.-C. F. Wang, "Learning deep latent space for multi-label classification," in *Proc. 31st AAAI Conf. Artif. Intell.*, 2017, pp. 2838–2844.
- [39] H. Coskun, F. Achilles, R. DiPietro, N. Navab, and F. Tombari, "Long short-term memory Kalman filters: Recurrent neural estimators for pose regularization," in *Proc. IEEE Int. Conf. Comput. Vis.*, 2017, pp. 5524–5532.
- [40] M. M. Islam, A. A. R. Newaz, and A. Karimoddini, "A pedestrian detection and tracking framework for autonomous cars: Efficient fusion of camera and LiDAR data," in *Proc. IEEE Int. Conf. Syst., Man, Cybern.*, 2021, pp. 1287–1292.
- [41] P. A. Lopes and M. Piedade, "The Kalman filter in active noise control," in *Proc. INTER-NOISE NOISE-CON Congr. Conf. Proc.*, 1999, pp. 1111–1124.
- [42] C. D. Petersen, R. Fraanje, B. S. Cazzolato, A. C. Zander, and C. H. Hansen, "A Kalman filter approach to virtual sensing for active noise control," *Mech. Syst. Signal Process.*, vol. 22, no. 2, pp. 490–508, 2008.
- [43] Z. Luo, D. Shi, W.-S. Gan, Q. Huang, and L. Zhang, "Performance evaluation of selective fixed-filter active noise control based on different convolutional neural networks," in *Proc. INTER-NOISE NOISE-CON Congr. Conf. Proc.*, 2023, pp. 1615–1622.
- [44] G. Huang, Z. Liu, L. V. D. Maaten, and K. Q. Weinberger, "Densely connected convolutional networks," in *Proc. IEEE Conf. Comput. Vis. Pattern Recognit.*, 2017, pp. 4700–4708.
- [45] W. Dai, C. Dai, S. Qu, J. Li, and S. Das, "Very deep convolutional neural networks for raw waveforms," in *Proc. IEEE Int. Conf. Acoust., Speech Signal Process.*, 2017, pp. 421–425.
- [46] Z. Luo, D. Shi, and W.-S. Gan, "A hybrid SFANC-FxNLMS algorithm for active noise control based on deep learning," *IEEE Signal Process. Lett.*, vol. 29, pp. 1102–1106, 2022.